

Direct-to-Device Connectivity for Integrated Communication, Navigation and Surveillance

Muhammad Asad Ullah*, Davi Brillhante[†], Luís Eduardo Partichelli Potrich^{†§},
José Suárez-Varela[‡], Paul Almasan[‡], Charles Cleary[†], Vadim Kramar*

*VTT Technical Research Centre of Finland, Finland

[†]ART, Collins Aerospace, Ireland

[‡]Telefonica Research, Spain

[§]Maynooth University, Ireland

Abstract—Sixth-generation (6G) communication systems are expected to support direct-to-device (D2D) connectivity, enabling standard user equipment (UE) to seamlessly transition to non-terrestrial network (NTN), particularly satellite communication mode, when operating beyond terrestrial network (TN) coverage. This D2D concept does not require hardware modifications to conventional UEs and eliminates the need for dedicated satellite ground terminals. D2D-capable UEs can be mounted on both manned and unmanned aircraft, however, they are especially well-suited for low-altitude unmanned aircraft due to their compact form factor, lightweight design, energy efficiency, and TN–NTN roaming capabilities. D2D can also enable beyond-visual-line-of-sight operation by providing NTN support for Communications, Navigation, and Surveillance (CNS) services during TN outages or congestion. This paper investigates the capabilities and limitations of D2D connectivity for low-altitude unmanned aircraft operating in urban environments. We analyze the variation in line-of-sight probability for both TN and NTN links as a function of aircraft altitude. We further compute path loss and received signal strength while accounting for a representative TN deployment with down-tilted antennas. The results show that the TN and NTN links complement each other, significantly improving the availability of the CNS service at low altitudes. These findings provide insights to support the design and optimization of future 6G-enabled integrated CNS services.

Index Terms—5G, 6G, aviation, CNS, D2D, NTN, UAS.

I. Introduction

Modern aircraft operations do not fully benefit from the use of 3rd generation partnership project (3GPP) technologies despite rapid advancements in the standards. The coverage of the cellular terrestrial network (TN) is optimized to serve users located at ground level and in the buildings, with down-tilted antennas [1], [2]. Non-terrestrial networks (NTN) address this challenge by extending wireless coverage to ground and aerial users, including the altitudes at which unmanned and manned aircraft operate [3], [4]. Moreover, NTNs are increasingly viewed as a native component of 6G networks, in which smart devices are expected to support both TN- and NTN-based cellular connectivity. This means 6G will benefit from the resources of both network segments to ensure service availability, continuity, ubiquity, and scalability [5].

Direct-to-device (D2D) connectivity is an emerging concept in 6G, where a standard consumer device, also called user equipment (UE), connects directly to a satellite when outside the TN coverage without needing any terrestrial base station (TBS) or ground satellite terminal [6], [7]. A D2D-capable UE can seamlessly switch between TN and NTN by leveraging its roaming capabilities [8], making it a promising approach to serve Unmanned Aircraft System (UAS) Traffic Management (UTM) with Communications, Navigation, and Surveillance (CNS) services.¹ This paves the way for implementing the Integrated CNS (ICNS) concept, which aims to deliver the ‘C’, ‘N’, and ‘S’ services jointly through the same technology stack [9], [10]. In addition to a wide range of applications, D2D-capable UEs will be able to establish TN and NTN links through the 3GPP stack to deliver ICNS services.

In the communications domain, UAS require low latency, high reliability, and continuous connectivity to support command-and-control (C2) operations and meet application-level data transmission requirements. By leveraging the complementary resources of TN and NTN, a UE with D2D functionalities can play a key role in ensuring uninterrupted ICNS service. For example, a UE mounted on an aircraft is expected to rely primarily on TN infrastructure to deliver CNS data. In the absence of terrestrial coverage, the UE can seamlessly switch to the NTN system, relying on low Earth orbit (LEO) satellites to maintain connectivity.

For navigation, stringent positioning accuracy requirements are currently under discussion for 6G systems. According to 3GPP TR 38.914 [11], the target positioning accuracy is 50 meters (m) for manned aircraft en-route operations, 10 m for its landing, and as low as 1 m for unmanned aircraft operations. 3GPP TR 22.870 [12] discusses accurate and latency positioning services for

This work has been accepted in IEEE 26th Integrated Communications, Navigation and Surveillance Conference, April 14–16, 2026, Herndon, Virginia, USA. Copyright has been transferred to IEEE.

¹Hereafter, we use the term aircraft to refer to those that operated at low-altitudes, including unmanned aircraft systems (UAS), vertical take-off and landing (VTOL)-capable aircraft (VCA), and general aviation, such as helicopters.

aircraft using hybrid TN–NTN technologies. A D2D-capable 6G UE can take advantage of hybrid TN–NTN connectivity to enable highly accurate positioning services, thus meeting the strict requirements of unmanned aircraft navigation and surveillance.

In terms of surveillance, a 6G UE equipped with D2D capabilities can enhance situational awareness in digital airspace by ensuring continuous and reliable connectivity, which is a key requirement for real-time aircraft monitoring and tracking [9].

The main contributions of this paper are as follows:

- We present an ICNS vision in which a UE mounted on an aircraft is equipped with D2D capabilities and can seamlessly roam between TN and NTN systems, thereby enhancing coverage availability and reliability by benefiting from network resources of both segments.
- We propose and develop a statistical framework to analyze and characterize the connectivity limits of TN and NTN systems while delivering ICNS services to an aircraft operating at low altitude in an urban environment.
- We validate the proposed framework over scenarios derived from relevant 3GPP technical reports and specifications. Particularly, we adopt 3GPP TR 38.811 [13], TR 36.814 [14], and TS 38.108 [15] to model path loss, vertical antenna gain, and receiver sensitivity thresholds, respectively. We then assess coverage by comparing the received signal strength indicator (RSSI) against sensitivity thresholds for both TN and NTN systems.

Overall, our results indicate that UEs with D2D capability and seamless roaming between TN and NTN provide a feasible solution for delivering ICNS services at low altitudes.

The remainder of this paper is organized as follows. In Section II we present the technical background and related works. In Sections III and IV, we describe our system model and discuss the results. Section V presents a discussion of the findings and highlights the key lessons learned. Finally, Section VI concludes this paper with final remarks.

II. Technical Background and Related work

This section discusses the studies on UAS and NTN channel modeling and recent developments of hybrid TN and NTN for the connectivity needs of UAS. Table I summarizes the key aviation acronyms and definitions used throughout the paper.

A. UAS and NTN channel modeling

3GPP has conducted investigations and specification works to enable connectivity for UAS, initially in LTE and later in 5G New Radio (NR). Early efforts in Release 15 focused on enhanced LTE support for aerial vehicles, captured in TR 36.777 [16], which defines evaluation

TABLE I
The list of key Aviation Acronyms and Definitions.

Acronyms	Definition
3GPP	3rd generation partnership project
5G	Fifth generation of cellular network technology
6G	Sixth generation of cellular network technology
A2A	Aircraft-to-aircraft
A2X	Aircraft-to-everything
A2G	Air-to-ground
ADS-B	Automatic dependent surveillance-broadcast
ACARS	Aircraft communications addressing and reporting system
C2	Command and control link
CDL	Clustered delay line
CNS	Communication, navigation and surveillance
CNPC	Command and non-payload communication
D2D	Direct-to-device
GNSS	Global navigation satellite system
ICNS	Integrated CNS
LoS	Line-of-sight
mmWave	millimeter wave
NTN	Non-terrestrial network
TBS	Terrestrial base stations
TDL	Tapped delay line
U-space	U-space airspace and digital services
UAS	Unmanned aircraft system
UTM	UAS traffic management
VCA	Vertical take-off and landing (VTOL) capable aircraft
VLL	Very low-level

scenarios, height-dependent propagation and line-of-sight (LoS) models, and identifies key interference and mobility challenges when serving unmanned aircraft with terrestrial base stations (TBSs) optimized for ground users. This report presents a channel model for user heights above the nominal ground level (typically 1.5 m), based on a UAS measurement campaign conducted across multiple field-trial configurations that vary the scenario, altitude, and mobility. Extensive results are provided in terms of reference signal received power (RSRP), reference signal received quality (RSRQ), and received signal strength indicator (RSSI).

Likewise, TR 38.811 [13] investigates channel and system aspects for NTN. For link-level simulations, it adopts reference Tapped delay line (TDL)/Clustered delay line (CDL) channel models and introduces elevation angle dependent LoS probabilities and path loss formulations, thus the LoS likelihood increases with elevation angle (90° means that the satellite is at Nadir angle) and UE environment type (from rural/suburban to dense urban). Although not focused on aerial users, this framework defines NTN system-level simulation guidelines under realistic propagation, and it has been widely used as a baseline for subsequent NTN channel modeling.

Beyond channel characterization, 3GPP has specified the services and architecture for UAS connectivity, identification, and tracking. In [9], the authors list 3GPP technical reports, specifications, and related work that define mechanisms for UAS registration, remote identification, user tracking via cellular infrastructure, and integration with external UAS traffic management (UTM/U-space) systems. A broader review of standardization efforts in [17] also highlights the work of other institutions, such as IEEE and ITU. These standardization efforts indicate

that current cellular systems are designed to support C2, telemetry, and identification services for UAS and low-altitude aircraft, although the focus is primarily on connectivity rather than on CNS requirements.

In parallel with standardization activities, academia has produced a rich body of work on analytical and simulation-based models for channel, propagation, and coverage analysis of unmanned aircraft communications. In [18], authors provide a survey of unmanned aircraft channel modeling, covering analytical, geometry-based, measurement-based, and stochastic approaches for A2G and A2A links over a wide range of frequencies and environments. This survey highlights the critical role of LoS probability, altitude-dependent path loss, and three-dimensional (3D) spatial modeling in capturing the unique characteristics of aircraft channels, including dynamic low-altitude mobility. It also emphasizes the gap between terrestrial channel models and aerial-user-focused models.

LoS probability modeling has been studied both analytically and empirically. In [19], the authors derive a compact elevation angle-dependent LoS probability in urban environments; the LoS probability increases with aircraft altitude and is parameterized by building height and density statistics, capturing the notion that obstacles cause less blockage as unmanned aircraft climb to higher altitudes. In [20], a study investigates a millimeter-wave (mmWave) unmanned aircraft communications scenario in urban-grid deployments. Their approach combines stochastic geometry with 3D building layouts to characterize the LoS probability for aerial users at different heights and street locations as a function of building density. In [21], a 3GPP UAS-focused channel model is applied to coverage analysis by comparing an analytically derived coverage probability model with Monte Carlo simulations based on the system model presented in [16]. The authors evaluate the impact of key system-model components, such as antenna array size, path loss, and LoS probability, and provide design recommendations, including the use of antenna arrays with fewer elements to extend coverage due to their larger beamwidth.

These works highlight the limitations of TN coverage models, tailored to ground users, and evidence that accurately capturing unmanned aircraft mobility remains an open challenge for both industry and academia. Reliable modeling depends critically on accurate representations of the underlying network, scenario, and LoS probability model. NTN emerges as a viable solution for coverage in situations where TN cannot achieve the desired signal quality; however, the channel models in the literature primarily focus on ground users. Extending 3GPP-based models with a detailed understanding of LoS probability, path loss, and coverage for unmanned aircraft communications is a viable approach to capture more diverse environments, deployment scenarios, and UAS dynamics, motivating the specialized modeling and design considered in this paper.

B. Coverage in the skies: Hybrid TN and NTN system

Typically, TN serves as the primary connectivity solution in areas with ground infrastructure. On the other hand, NTN and, especially, satellites extend coverage to remote and oceanic areas [5]. Beyond coverage extension, NTN can also complement TN in dense urban environments by managing excess traffic during peak-demand periods. Furthermore, in the event of TN failures, satellite links can maintain service continuity, thereby improving overall system resilience [1]. Hybrid TN and NTN enables the delivery of ICNS services anywhere at any time [9].

1) Terrestrial network: When TN infrastructure is present, TBS can provide an aircraft connection to deliver CNS services. In addition, TN can also enable Internet connectivity on VCA for passengers and onboard systems. It is worth mentioning that current TBS deployments are primarily optimized for ground users rather than aerial platforms [21], [22].

2) Non terrestrial network: In legacy CNS, satellite communication is an important component of aeronautical communications in oceanic and remote environments. For decades, satellites have provided a communication bridge between aircraft and ground systems [23]. Table II shows the satellite technologies, constellation and their CNS services. For example, satellite-based aeronautical communication systems introduced in the early 1990s have supported voice and data services, including ACARS and ADS-B messaging. With rapid advancements in satellite technology, especially LEO constellations, NTN coverage is expanding beyond remote regions to include urban environments. This evolution enables NTN to complement TN not only in coverage-limited areas but also during network congestion or outages in urban areas [9].

3) Integrated TN and NTN system: A combination of cellular TN and proprietary NTN can be used for delivering CNS services to an unmanned aircraft flying at low altitude. However, this implementation may require two separate transceivers for TN and NTN systems [4], [24], which can be challenging for small platforms with strict size, weight, and power constraints. Existing studies highlight that combining 3GPP cellular TN and NTN systems can significantly improve service availability, reliability, and coverage continuity [5], [25]. To realize the ICNS vision, hybrid TN and NTN systems can support aircraft operations across wide geographic regions and at different altitudes, from very low-level (VLL) to high-altitude airspace [9].

In future communication systems, D2D capabilities will allow commercial off-the-shelf UE to transition seamlessly between terrestrial and satellite links without requiring dedicated satellite hardware [7], [26], [27]. This capability significantly simplifies the use of TN and NTN, and broadens the applicability of hybrid architectures for aviation use cases, especially for delivering ICNS services to unmanned aircraft.

TABLE II
Existing NTN technologies and their CNS services.

Technology	Constellation	Category
Classic Aero	Viasat (Inmarsat)	Communication Surveillance
SwiftBroadband-Safety	Viasat (Inmarsat)	Communication Surveillance
Iridium Certus	Iridium	Communication
Space-based ADS-B	Iridium (Aireon)	Surveillance
GNSS	GPS, GLONASS Galileo, BeiDou	Navigation enables Surveillance

TABLE III
5G NTN bands for uplink and downlink.

NR band	Uplink	Downlink
n253	1668 – 1675 MHz	1518 – 1525 MHz
n254	1610 – 1626.5 MHz	2483.5 – 2500 MHz
n255	1626.5 – 1660.5 MHz	1525 – 1559 MHz
n256	1980 – 2010 MHz	2170 – 2200 MHz
n510	27.5 – 28.35 GHz	17.7 – 20.2 GHz
n511	28.35 – 30 GHz	17.7 – 20.2 GHz
n512	27.5 – 30 GHz	17.7 – 20.2 GHz

C. Spectrum bands for TN and NTN

3GPP 5G NR operates across multiple frequency ranges (FRs) for terrestrial networks. These ranges include FR1 and FR2, as well as the upper mid-band, often referred to as FR3. FR1 spans 410–7125 MHz and is widely used because it offers a practical balance between coverage and capacity. FR3 fills the gap between FR1 and FR2 by operating in the 7–24 GHz band, which is better suited to more localized, high-capacity deployments. FR2 covers 24.25–52.6 GHz, enabling much higher data rates, but usually with shorter range and stronger sensitivity to blockage [28]. In an urban aerial scenario with operations in low altitudes, propagation differs from that of typical ground users [29]. In FR1, airborne UEs often have LoS to several base stations, thereby increasing inter-cell interference. FR2 links rely on narrower beams, which can reduce unwanted visibility and help manage interference, although coverage continuity is more challenging in dense urban areas. FR2 and FR3 links may require very-small-aperture terminals, while L/S bands in FR1 are suitable for D2D connectivity [30], [31].

NTN communication uses satellite bands specified in 3GPP TS 38.101-5 [32] and summarized in Table III. The spectrum includes FR1 NTN from 410–14500 MHz and FR2 NTN from 10.7–30 GHz. Several NTN bands overlap in frequency because spectrum allocations differ across regions. This overlap can simplify device design and support multi-region operation. Lower frequencies, such as the L and S bands, have lower propagation loss and are better suited to compact terminals, but they typically offer limited bandwidth. This constrains throughput for data-intensive UAS services, such as real-time video streaming. Although this limited bandwidth may satisfy current ICNS requirements, it may become insufficient as aircraft density increases in the future. Higher-frequency options, such as the Ku and Ka bands, offer larger bandwidths and higher throughput. However, these bands are more sensitive to atmospheric conditions. For example, Starlink operates in the Ku band, where rain and high humidity can reduce performance [33]. As a result, operating in these bands typically requires high-gain directional antennas, which can be too large and heavy for small unmanned aircraft. In addition, satellite receivers operating in these bands require high antenna gain to overcome the substantial

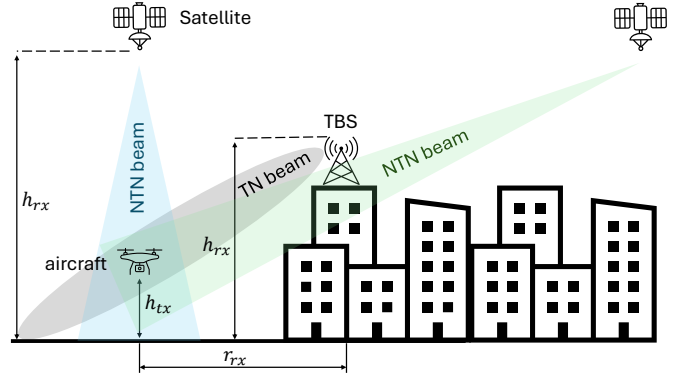


Fig. 1. Illustrations of unmanned aircraft operation in urban environment using TN and NTN systems.

path loss [7]. Therefore, we consider the L- and S-bands more suitable candidates for D2D links supporting ICNS services.

III. System Model

This section presents the mathematical modeling for LoS probability, path loss, vertical radiation pattern of the antennas, and analytical formulation for computing the received signal strength. Fig. 1 presents a high-level illustration of our scenario. Table IV shows the key notations and their definitions. We investigate an urban scenario in which a TBS is installed on a building rooftop at a height (h_{rx}) above ground level (AGL). An aircraft is located at a height (h_{tx}) AGL, at a horizontal distance (r_{tx}) from the TBS. We also consider an NTN system with a LEO satellite orbiting the Earth at a height (h_{rx}) AGL, whose elevation angle varies between 10° and 90° due to the satellite's orbital motion.

A. Line-of-Sight Probability Model

In this paper, we calculate LoS probability using the ITU-R P.1410-6 statistical model (refer to Section 2.1.4 statistical model in [34]). This model requires three parameters, including: (i) α defines the ratio of built-up area to the total site area (dimensionless); (ii) β is the mean building density, measured in buildings per square kilometer, and (iii) γ defines the building-height distribution, assumed to follow a Rayleigh distribution. If we assume that buildings are placed evenly in a grid, a

TABLE IV
The list of key notations and their definitions.

Acronyms	Definition
α	Ratio of built-up area to the total site area
β	Mean building density measured as buildings/km ²
γ	Building height distribution
b_1	Number of buildings passed per kilometer
b_r	Number of buildings crossed in ray path
d_i	Buildings distances
h_i	Ray height at the distance d_i
P_L	Total path loss
$P_{L_{LoS}}$	LoS path loss
$P_{L_{NLoS}}$	NLoS path loss
δ_r	Separation between the buildings
\mathbb{P}_{LoS}	Line-of-sight (LoS) probability

one-kilometer ray would pass over $\sqrt{\beta}$ buildings. However, since only a ratio α of the land is actually covered with buildings, the number of buildings crossed per kilometer is reduced accordingly as

$$b_1 = \sqrt{\alpha\beta} \quad (1)$$

Ray path (r_{rx}), also known as ground range, is a two-dimensional horizontal distance between the transmitter and the receiver. The unit of r_{rx} is a kilometer. The total number of buildings crossed over a ray path (r_{rx}) is given by

$$b_r = \lfloor r_{rx} b_1 \rfloor \quad (2)$$

where (2) uses the floor function ($\lfloor \cdot \rfloor$) to ensure that the output is an integer number. In the next step, ITU-R P.1410-6 statistical model [34] assumes that the buildings are evenly spaced between the transmitter and the receiver, where each building is located at a distance (d_i) as follows

$$d_i = \left(i + \frac{1}{2}\right) \delta_r, \quad i \in \{0, 1, \dots, (b_r - 1)\} \quad (3)$$

where $\delta_r = \frac{r_{rx}}{b_r}$ is the separation between the buildings. The variable d_i denotes the horizontal distance from the transmitter to the potential blockage point on the i -th building. At this distance, h_i corresponds to the height of the ray at the obstruction point as

$$h_i = h_{tx} - \frac{d_i (h_{tx} - h_{rx})}{r_{rx}} \quad (4)$$

where parameters h_{tx} and h_{rx} denote the heights of the transmitter (aircraft) and receiver (TBS or satellite) AGL, respectively. At a horizontal distance d_i , the term P_i represents the probability that the building height does not exceed ray height h_i , i.e., the probability that the building height is less than ray height h_i . Thus, the probability P_i is given by

$$P_i = 1 - \exp\left(-\frac{h_i^2}{2\gamma^2}\right) \quad (5)$$

The $P_{LoS,i}$ represents probability of having a LoS path at distance d_i as

$$\mathbb{P}_{LoS,i} = \prod_{j=0}^i P_j, \quad j \in \{0, \dots, i\} \quad (6)$$

B. Path loss Model

The total path loss is expressed as the weighted combination of LoS and non-line-of-sight (NLoS) components, where the weights correspond to their respective occurrence probabilities as in [35]. Specifically, it is given by the sum of the product of the LoS probability and the LoS path loss, as well as the product of the NLoS probability and the NLoS path loss. The total path loss is modeled as

$$P_L = \mathbb{P}_{LoS} \times P_{L_{LoS}} + (1 - \mathbb{P}_{LoS}) \times P_{L_{NLoS}} \quad (7)$$

Similar to 3GPP TR 38.811 [13], LoS path loss is defined by

$$P_{L_{LoS}} = 32.45 + 20 \log_{10}(f_c) + 20 \log_{10}(r) + SF \quad (8)$$

where carrier frequency (f_c) in GHz, r in m is link distance, also called slant range, and SF denotes the shadow fading component. Following 3GPP TR 38.811 [13], path loss for NLoS ray is calculated as

$$P_{L_{NLoS}} = 32.45 + 20 \log_{10}(f_c) + 20 \log_{10}(r) + SF + CL \quad (9)$$

where CL represents the clutter loss. Unlike the path loss for a ray under perfect LoS conditions, NLoS propagation incurs additional attenuation due to clutter loss CL, caused by blockages such as surrounding buildings and ground obstacles. Note that the clutter-loss model in 3GPP TR 38.811 [13] assumes a user at ground level. In this paper, we adopt an altitude-dependent clutter attenuation model to account for the aircraft's variable height, which ranges from 1 to 300 m. Particularly, the clutter loss is modeled as an exponentially decaying function of the aircraft height as

$$CL = CL_{\max} \exp(-h_{tx}/h_0) \quad (10)$$

where CL_{\max} is the maximum clutter loss, and $h_0 = 1.25 \times \gamma$ m represents building height. In (10) formulation reflects the reduction of clutter effects as the aircraft rises above the urban infrastructure.

In (8) and (9), r is link distance (slant range) between transmitter (aircraft) and receiver (TBS or satellite). In case of TN, link distance between aircraft and TBS is calculated as $r = \sqrt{(r_{rx} \times 1000)^2 + |h_{tx} - h_{rx}|^2}$. In case of NTN, we consider a satellite as a receiver and aircraft as a transmitter. We calculate link distance using the MATLAB built-in function $r = \text{height2range}(\text{tgtht}, \text{anht}, \text{el})^2$ which converts a target height to propagated range, where tgtht is receiver height as $h_{rx} = 300,000$ m, anht is variable transmitter (aircraft) height between 1 to 300 m, and

²<https://se.mathworks.com/help/radar/ref/height2range.html>

el is the elevation angle between aircraft and satellite. Similarly, in the case of NTN, we calculate r_{rx} , which is a two-dimensional distance also called ground range between aircraft and satellite using the MATLAB built-in function as $r_{rx} = \text{height2grndrange}(\text{tgtht}, \text{anht}, \text{el})^3$.

C. Vertical antenna pattern

In 3GPP TR 36.814 [14], the vertical antenna pattern in dB is defined by the antenna downtilt angle, half-power beamwidth, and the minimum vertical gain as

$$A_V(\theta) = -\min \left[12 \left(\frac{\theta - \theta_{\text{etilt}}}{\theta_{3\text{dB}}} \right)^2, SLA_V \right] \quad (11)$$

where $\theta_{3\text{dB}}$ is the half-power beamwidth, SLA_V in dB is minimum vertical gain, θ_{etilt} is electrical antenna downtilt angle, and $\theta \in [-90^\circ, 90^\circ]$ is the elevation angle. However, the actual angle experienced by the aircraft depends on TBS height h_{tx} , aircraft height h_{tx} , and link distance r . We calculate angle θ using the MATLAB built-in function `height2el`⁴.

D. Received signal power

We use the Friis transmission formula [36] to calculate the received power in dB as

$$P_{rx} = P_{tx} + G_{tx} + G_{rx} + A_V - P_L \quad (12)$$

where P_{tx} , G_{tx} , G_{rx} , A_V , and P_L denote the transmit power, transmitter antenna gain, receiver antenna gain, vertical antenna gain, and path loss, respectively. Horizontal antenna pattern is not explicitly modeled; instead, we consider a best-case condition assuming TBS to be horizontally omnidirectional as in [22]. For the NTN scenario, the satellite antenna radiation pattern is assumed to remain uniform within a given spot beam and independent of the aircraft altitude. Consequently, the vertical antenna pattern A_V is neglected in the NTN analysis.

IV. Results

A. Evaluation setup

Table V lists the key parameters and their values used in our evaluation. Specifically, we consider an urban scenario with $\alpha = 0.3$, $\beta = 500$, and $\gamma = 15$ [35]. We consider a 6G UE with D2D capabilities mounted on the aircraft, transmitting at 23 dBm and using an antenna with 0 dBi gain. We assume the TBS is installed at the height (h_{rx}) of 25 m. TBS carrier frequency (f_c) is 3.6 GHz and it features a receiving antenna with gain $G_{rx} = 8$ dBi, half-power beamwidth ($\theta_{3\text{dB}} = 10^\circ$, electrical antenna downtilt ($\theta_{\text{etilt}} = 6^\circ$, and minimum vertical gain ($SLA_V = 20$ dB [14], [22]. We consider the reference receiver sensitivity is approximately -100

³<https://se.mathworks.com/help/radar/ref/height2grndrange.html>

⁴<https://se.mathworks.com/help/radar/ref/height2el.html>

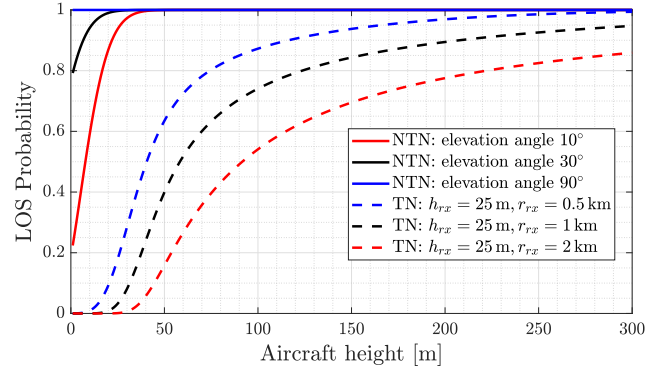


Fig. 2. LoS probability as a function of aircraft height above the ground.

dBm for operation at $f_c = 3.6$ GHz with 5 MHz channel bandwidth and 15 kHz subcarrier spacing (SCS) [37].

For the NTN segment, we assume a satellite orbiting at height (h_{rx}) of 300,000 m, which features a higher antenna gain $G_{rx} = 38$ dBi to compensate for extreme path loss. Recent advancements in satellite communications have demonstrated the feasibility of high-gain satellite antennas for D2D connectivity [7]. For example, AST SpaceMobile is developing LEO satellite systems capable of directly connecting to standard 5G mobile devices without hardware modification. These systems operate in frequency bands comparable to conventional terrestrial cellular bands. Reported uplink frequencies include 846.5–849 MHz, 845–846.5 MHz, and 788–798 MHz, while downlink operation includes 891.5–894 MHz, 890–891.5 MHz, and 758–768 MHz. The satellite payload employs electronically steerable beams and achieves a maximum antenna gain on the order of 36 dBi [38].

Similarly, Starlink has initiated direct-to-cell services supporting 4G connectivity in collaboration with T-Mobile, utilizing spectrum in the 1910–1915 MHz and 1990–1995 MHz bands. Publicly available information indicates peak satellite antenna gains of approximately 38 dBi for such systems [39]. In addition, system-level evaluations reported in 3GPP TR 38.821 [40] consider satellite antenna gains as high as 51 dBi for S-band (2 GHz) NTN scenarios. These examples support the assumption of high satellite antenna gain in our link budget analysis. Furthermore, in the NTN case, we set the receiver sensitivity threshold for a channel with 5 MHz bandwidth at 15 kHz subcarrier spacing (SCS), which is -102.4 dBm as in 3GPP TS 38.108 [15].

B. Numerical results

In our evaluation, we consider a range of scenarios for the TN and NTN segments (see Fig. 1). For the TN case, we evaluate cases with several horizontal distances $r_{rx} \in [0.5, 1, 2]$ km, while for the NTN case, we consider elevation angles $\text{el} \in [10^\circ, 30^\circ, 90^\circ]$ between the aircraft

TABLE V
Key parameters used in the evaluation.

Parameter	Value
Common Parameters	
α	0.3
β	500 buildings/km ²
γ	15 m
Aircraft height (h_{tx})	1–300 m
Bandwidth	5 MHz
LoS shadow fading (SF)	4 dB
Maximum clutter loss (CL_{max})	34.3 dB
NLoS shadow fading (SF)	6 dB
Receiver sensitivity	-102.4 dBm
UE antenna gain (G_{tx})	0 dBi
UE transmit power (P_{tx})	23 dBm
TN Parameters	
Carrier frequency (f_c)	3.6 GHz
Electrical antenna downtilt (θ_{etilt})	6°
TBS antenna gain (G_{rx})	8 dBi
TBS height (h_{rx})	25 m
TBS half-power beamwidth (θ_{3dB})	10°
Vertical antenna gain (SLA_V)	20 dB
NTN Parameters	
Carrier frequency (f_c)	2 GHz
Receiver antenna gain (G_{rx})	38 dBi
Satellite altitude (h_{rx})	300 km
Satellite elevation angles	10°, 30°, 90°
Satellite orbit	Very LEO

and the satellite, covering a wide range of possible configurations.

LoS probability: Fig. 2 illustrates the LoS probability for TN and NTN connections as a function of the aircraft height (h_{tx}). The TN link exhibits a significantly lower LoS probability compared with all three NTN cases corresponding to elevation angles of 10°, 30°, and 90°. This difference arises because, in the TN scenario, the TBS is located at a height of $h_{rx} = 25$ m AGL, whereas the NTN scenario considers a LEO satellite at an altitude of $h_{rx} = 300,000$ m. Consequently, the link distance (slant range), denoted by r , between the aircraft and the satellite encounters fewer obstacles than in the case of communication with a TBS. As the aircraft moves farther from the TBS, the horizontal distance r_{rx} increases, which reduces the ray slope and increases the number of blockages, thereby reducing the LoS probability. Specifically, in the TN case, when $r_{rx} = 0.5$ km, the LoS probability is approximately 0.5 at an aircraft height of 40 m. In contrast, for $r_{rx} = 2$ km, the LoS probability remains close to zero until the aircraft height (h_{tx}) reaches about 30 m, and it increases to 0.5 at $h_{tx} = 90$ m. At the maximum aircraft height of 300 m, the LoS probabilities are approximately 0.99, 0.94, and 0.85 for $r_{rx} = 0.5, 1,$ and 2 km, respectively.

In the NTN scenario, when the aircraft height is 10 m, the LoS probabilities are approximately 0.58, 0.94, and 1 for elevation angles of 10°, 30°, and 90°, respectively. The LoS probability is close to one when the aircraft height exceeds 40 m AGL for all three NTN cases.

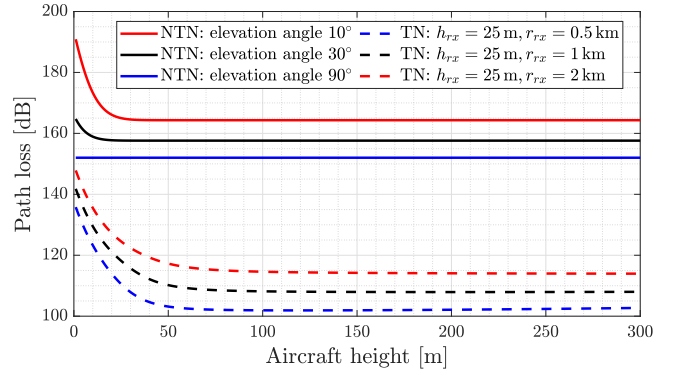


Fig. 3. Path loss as a function of aircraft height above the ground level.

Path loss: We further use the LoS results from Fig. 2 to derive the path loss as a function of the aircraft height AGL, using (7). Fig. 3 illustrates the resulting path loss. As expected, the TN connection exhibits significantly lower path loss than the NTN connection due to the shorter link distance r between the aircraft and the TBS. Specifically, when the aircraft is close to ground level, the TN link experiences path losses of 135 dB, 141 dB, and 147 dB for distances between the aircraft and TBS of $r_{rx} = 0.5, 1,$ and 2 km, respectively. The path loss decreases sharply to 103 dB, 110 dB, and 117 dB as the aircraft height increases to 50 m.

In the NTN case, a LEO satellite at an altitude of $h_{rx} = 300,000$ m is considered, resulting in link distances r of 1237 km, 572 km, and 300 km at elevation angles of 10°, 30°, and 90°, respectively. At an elevation of 90°, the satellite is assumed to be directly above the aircraft, resulting in a perfect LoS condition; hence, according to our model the path loss remains constant at 152 dB for all aircraft heights. In contrast, the NTN case with an elevation angle of 10° exhibits a path loss exceeding 174 dB when the aircraft height is 10 m, where the NLoS component is dominant, leading to high clutter losses. After the aircraft height exceeds 30 m, the path loss stabilizes at approximately 164 dB. For the NTN scenario with an elevation angle of 30°, the path loss is 158 dB when the aircraft altitude reaches 10 m. To compensate for these high path losses, we assume that the satellite has a higher receive antenna gain of $G_{rx} = 38$ dBi.

Vertical antenna gain: As mentioned earlier, the coverage of the cellular TBS is optimized to serve users at ground level [14]. This is achieved through antenna downtilting [22]. Fig. 4 shows the vertical antenna gain pattern when the electrical antenna downtilt $\theta_{etilt} = 6^\circ$. In Fig. 4, the blue curve represents the overall vertical antenna gain pattern, while the red curve shows the gain experienced by a UE mounted on the aircraft. It can be observed that the magnitude of the experienced gain decreases as the aircraft moves farther away from the TBS.

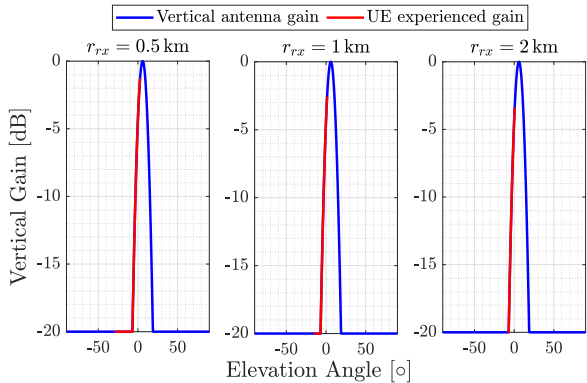


Fig. 4. Impact of down tilting on the vertical antenna gain.

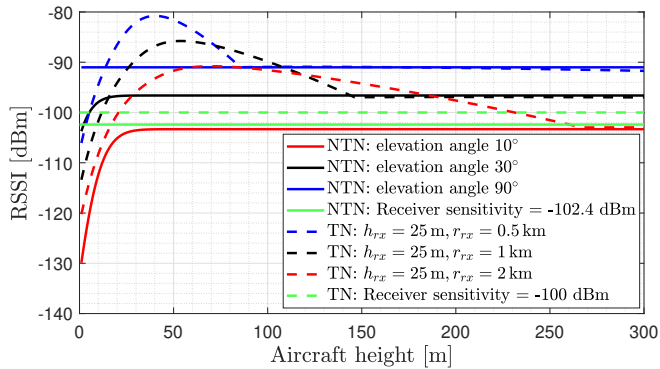


Fig. 5. Received signal strength indicator as a function of aircraft height.

Coverage: Note that, for a channel bandwidth of 5 MHz and SCS of 15 kHz, the receiver sensitivity requirements are -100 dBm and -102.4 dBm for TN and NTN connections, respectively. A RSSI above these receiver sensitivity thresholds is required to successfully establish a connection between the UE and the TBS or satellite. Fig. 5 illustrates the RSSI as a function of aircraft height for both TN and NTN connections. When the aircraft is at $r_{rx} = 0.5, 1,$ and 2 km from the TBS, a TN connection is feasible only when the aircraft altitude h_{tx} exceeds 5, 12, and 20 m, respectively. For $r_{rx} = 2$ km, the link between the aircraft and the TBS enters outage when h_{tx} goes above 230 m.

In the NTN case, connectivity at an elevation angle of 90° is feasible regardless of aircraft height, while at 30° it becomes feasible when the aircraft height exceeds 3 m. However, the NTN link with an elevation angle of 10° fails to establish a connection across the entire aircraft height range. Communication at 10° can become feasible above 25 m if the satellite receiving antenna gain G_{rx} is further increased by 2 dBi to 40 dBi.

V. Discussion

As described in Section II-B, TNs typically serve as the primary connectivity solution in areas with ground infrastructure. On the other hand, NTNs, especially

satellites, extend coverage to remote and oceanic areas. Beyond coverage extension, NTNs can also complement TNs in dense urban environments by managing excess traffic during peak-demand periods. Furthermore, in the event of terrestrial network failures, satellite links can maintain service continuity, thereby improving overall system resilience.

As illustrated in Fig. 5, for a TN with a network density that results in the horizontal distance from any TBS to aircraft less than or equal to $r_{rx} = 0.5$ km, the TN coverage would ensure an RSSI that is above the minimum receiver sensitivity threshold. Since most urban commercial TNs will have high TBS densities, which would result in much shorter horizontal distances between aircraft and TN base stations, the general use of TNs for low altitude below 300 m would become feasible for primary connectivity purposes. The access to multiple TBSs can be provisioned via access roaming agreements with multiple local or regional TN service providers, such as commercial Mobile Network Operators (MNOs). Through agreements with multiple NTNs and multiple MNOs, a very resilient combined NTN and TN system can be feasibly established.

Beyond densified TN coverage areas, where TBS may be more than $r_{rx} = 0.5$ km of horizontal distance from an aircraft, Fig. 5 also shows the potential for NTN to provide the RSSI required to meet or exceed the minimum receiver sensitivity threshold, when the elevation angle of an aircraft to a serving satellite is near 30° or higher. This shows the feasibility of a combined TN and NTN system to both provide extended coverage where TN coverage is limited or unavailable, and it shows that a combined TN and NTN system can support an increased volume of aircraft via the enhancement (augmentation) of TN capacity with NTN capacity. State-of-the-art commercial mobile networks often have network density that ensures distances to macro or micro base stations are within hundreds of meters. Therefore, the overall results demonstrate that the combined TN and NTN system can provide the extended coverage required to deliver ICNS services at low altitudes.

VI. Conclusion

This paper presents a vision for integrated Communication, Navigation, and Surveillance relying on hybrid TN–NTN connectivity in 6G networks. This concept assumes that a 6G user equipment with satellite-based direct-to-device capabilities is mounted on an aircraft, enabling it to leverage both terrestrial and non-terrestrial network resources. This can add significant system redundancy, ensuring overall network availability and system resilience. The combined use of terrestrial and non-terrestrial networks enhances coverage availability for CNS services at altitudes where TN coverage is limited or unavailable. This paper concludes that a UE with D2D capability and the ability to smoothly roam between TN and NTN can

provide a feasible solution for using combined networks to support CNS services at low altitude. The results of the modeling and simulation illustrate that a combined TN and NTN system, particularly one operating in an urban environment, can enable low-altitude CNS services to be provisioned with the primary connectivity, extended coverage, and resilience needed to deliver connectivity for ICNS services for low-altitude operation. In future work, we plan to investigate satellite-based device-to-device communication to enable aircraft-to-aircraft and aircraft-to-everything communication via satellite, without relying on feeder links or ground stations. As another future research direction, we plan to investigate the feasibility of extending terrestrial base-station coverage to low-altitude aerial corridors using up-tilted antennas. These aerial corridors are defined by aviation authorities. Our goal is to optimize network performance specifically within these predefined corridors, rather than extending coverage everywhere. This targeted approach will focus on improving the quality and reliability of ICNS services for aerial operations along designated aerial corridors. Our NTN results indicate that communication with LEO satellites is not feasible at low elevation angles. In the future, we also aim to conduct a comprehensive study of this issue by analyzing different satellite constellation densities, ranging from a few hundred to several thousand satellites. This investigation will help us better understand the impact of constellation size on link feasibility and overall system performance.

Acknowledgment

This work has been performed under the ANTENNAE project, which has received funding from SESAR3 Joint Undertaking under the European Union's HORIZON-SESAR-2023-DES-ER-02 topic, Grant Agreement No. 101167288. However, the views and opinions expressed are those of the authors only and do not necessarily reflect those of the European Union or SESAR 3 JU. Neither the European Union nor the SESAR 3 JU can be held responsible for them. The authors acknowledge the use of ChatGPT for proofreading and grammatical improvements in the preparation of this manuscript.

References

- [1] M. Benzaghta, G. Geraci, R. Nikbakht, and D. López-Pérez, "UAV communications in integrated terrestrial and non-terrestrial networks," in *GLOBECOM 2022 - 2022 IEEE Global Communications Conference*, 2022, pp. 3706–3711.
- [2] L. Chen, M. A. Kishk, and M.-S. Alouini, "Dedicating cellular infrastructure for aerial users: Advantages and potential impact on ground users," *IEEE Transactions on Wireless Communications*, vol. 22, no. 4, pp. 2523–2535, 2023.
- [3] V. Leon, I. Christofilos, A. Nesiadis, I. Paraskevas, J. Perrela, G. Ioannopoulos, A. Tasoulis-Nonikas, M. Bernou, and J. Reading, "Towards enabling 5G-NTN satellite communications for manned and unmanned rotary wing aircraft," in *2024 IEEE 29th International Workshop on Computer Aided Modeling and Design of Communication Links and Networks (CAMAD)*, 2024, pp. 1–6.

- [4] M. Figaro, F. Rossato, A. Bonora, M. Giordani, G. Schembra, and M. Zorzi, "Experimental evaluation of a UAV-mounted LEO satellite backhaul for emergency connectivity," 2026. [Online]. Available: <https://arxiv.org/abs/2601.03958>
- [5] G. Araniti, A. Iera, S. Pizzi, and F. Rinaldi, "Toward 6G non-terrestrial networks," *IEEE Network*, vol. 36, no. 1, pp. 113–120, 2022.
- [6] H. B. Pasandi, J. A. Fraire, S. Ratnasamy, and H. Rivano, "A survey on direct-to-device satellite communications: Advances, challenges, and prospects," in *Proceedings of the 2nd International Workshop on LEO Networking and Communication*, 2024, pp. 7–12.
- [7] M. Asad Ullah, C. D. Gedara, A. Anttonen, A. Sethi, M. D. Khattak, M. Höyhty, J. Wigard, and K. Mikhaylov, "3GPP RedCap non-terrestrial networks: Direct-to-device feasibility study," *Authorea Preprints*, 2025.
- [8] European Space Agency, "Direct-to-device (D2D) satellite communications – space for 5G/6G & sustainable connectivity," <https://connectivity.esa.int/artes-4-0-programme-overview/space-for-5g-6g-sustainable-connectivity/direct-to-device-d2d>, 2026, accessed: 2026-03-02.
- [9] M. Asad Ullah et al., "5G integrated communications, navigation, and surveillance: A vision and future research perspectives," in *2025 Integrated Communications, Navigation and Surveillance Conference (ICNS)*, 2025, pp. 1–13.
- [10] H. Alshaer, A. Ganau, D. Brillhante, C. Cleary, M. A. Ullah, and V. Kramar, "Next-generation integrated communications, navigation, and surveillance services," in *2025 Integrated Communications, Navigation and Surveillance Conference (ICNS)*, 2025, pp. 1–10.
- [11] 3rd Generation Partnership Project (3GPP), "Study on 6G scenarios and requirements," 3GPP, Technical Report (TR) 38.914, 2025, draft, Release 19. [Online]. Available: <https://portal.3gpp.org/desktopmodules/Specifications/SpecificationDetails.aspx?specificationId=4392>
- [12] —, "Study on 6G use cases and service requirements," 3GPP, Technical Report (TR) 22.870, 2025, draft, Release 20. [Online]. Available: <https://portal.3gpp.org/desktopmodules/Specifications/SpecificationDetails.aspx?specificationId=4374>
- [13] —, "3GPP TR 38.811: Study on New Radio (NR) to support non-terrestrial networks," 3GPP, Technical Report 38.811, 2020, release 15. [Online]. Available: <https://portal.3gpp.org/desktopmodules/Specifications/SpecificationDetails.aspx?specificationId=3234>
- [14] —, "3GPP TR 36.814: Evolved Universal Terrestrial Radio Access (E-UTRA); Further advancements for E-UTRA physical layer aspects," <https://portal.3gpp.org/desktopmodules/Specifications/SpecificationDetails.aspx?specificationId=2493>, 3GPP, Technical Report 36.814, 2010, release 9.
- [15] —, "NR; Satellite Access Node Radio Transmission and Reception," 3GPP, Technical Specification (TS) 38.108, 2022, release 17, under change control. [Online]. Available: <https://portal.3gpp.org/desktopmodules/Specifications/SpecificationDetails.aspx?specificationId=3934>
- [16] —, "3GPP TR 36.777: Study on Enhanced LTE Support for Aerial Vehicles," 3GPP, Technical Report 36.777, 2018, release 15. [Online]. Available: https://www.3gpp.org/ftp/Specs/archive/36_series/36.777/
- [17] A. S. Abdalla and V. Marojevic, "Communications standards for unmanned aircraft systems: The 3GPP perspective and research drivers," *IEEE Communications Standards Magazine*, vol. 5, no. 1, pp. 70–77, 2021.
- [18] A. A. Khuwaja, Y. Chen, N. Zhao, M.-S. Alouini, and P. Dobbins, "A Survey of Channel Modeling for UAV Communications," *IEEE Communications Surveys & Tutorials*, vol. 20, no. 4, pp. 2804–2821, 2018.
- [19] A. Al-Hourani, "On the probability of line-of-sight in urban environments," *IEEE Wireless Communications Letters*, vol. 9, no. 8, pp. 1178–1181, 2020.
- [20] M. Gapeyenko, D. Moltchanov, S. Andreev, and R. W. Heath, "Line-of-sight probability for mmWave-based uav communications in 3D urban grid deployments," *IEEE Transactions on Wireless Communications*, vol. 20, no. 10, pp. 6566–6579, 2021.

- [21] Z. Cui et al., "Coverage analysis of cellular-connected uav communications with 3gpp antenna and channel models," in 2021 IEEE Global Communications Conference (GLOBECOM), 2021, pp. 1–6.
- [22] N. Cherif and Q.-U.-A. Nadeem, "Merits of serving uavs via terrestrial networks: A vertical antenna radiation study," in ICC 2025 - IEEE International Conference on Communications, 2025, pp. 1470–1475.
- [23] N. Mäurer, T. Guggemos, T. Ewert, T. Gräupl, C. Schmitt, and S. Grundner-Culemann, "Security in digital aeronautical communications a comprehensive gap analysis," *International Journal of Critical Infrastructure Protection*, vol. 38, p. 100549, 2022. [Online]. Available: <https://www.sciencedirect.com/science/article/pii/S187454822200035X>
- [24] A. Ramírez-Arroyo, T. B. Sørensen, and P. Mogensen, "Terrestrial 5G and Starlink ntn multi-connectivity toward 6G communications integration era: An empirical assessment," *IEEE Open Journal of the Communications Society*, vol. 6, pp. 5269–5283, 2025.
- [25] F. Rinaldi, H.-L. Maattanen, J. Torsner, S. Pizzi, S. Andreev, A. Iera, Y. Koucheryavy, and G. Araniti, "Non-terrestrial networks in 5G & beyond: A survey," *IEEE access*, vol. 8, pp. 165 178–165 200, 2020.
- [26] H. Taha, P. Vári, and A. Lapsánszky, "Direct-to-device satellite communications in the European Union: Spectrum allocation and regulatory pathways within the ITU framework," *IEEE Access*, vol. 13, pp. 190 556–190 581, 2025.
- [27] F. Wang, S. Zhang, E.-K. Hong, and T. Q. S. Quek, "Constellation as a service: Tailored connectivity management in direct-satellite-to-device networks," *IEEE Communications Magazine*, vol. 63, no. 11, pp. 30–36, 2025.
- [28] R. Dilli, "Analysis of 5G wireless systems in FR1 and FR2 frequency bands," in 2020 2nd International Conference on Innovative Mechanisms for Industry Applications (ICIMIA), 2020, pp. 767–772.
- [29] S. J. Seah, S. L. Jong, H. Y. Lam, and C. Y. Leow, "Evaluation of UAV communication performance in urban environment: A study on air-to-ground propagation factors," in 2025 IEEE 17th Malaysia International Conference on Communication (MICC), 2025, pp. 1–6.
- [30] T. S. Rappaport, T. E. Humphreys, and S. Nie, "Spectrum opportunities for the wireless future: From direct-to-device satellite applications to 6G cellular," *npj Wireless Technology*, vol. 1, no. 1, p. 8, 2025.
- [31] A. Yastrebova-Castillo, S. Tocklin, H. Kokkinen, M. A. Ullah, M. Höyhty, and M. Majanen, "Integrated UAS-satellite communications in 6G: An overview," in Proceedings of the 15th EASN International Conference, 2024, accepted for publication.
- [32] 3rd Generation Partnership Project (3GPP), "NR; User Equipment (UE) radio transmission and reception; Part 5: Satellite access Radio Frequency (RF) and performance requirements," 3GPP, Technical Report 38.101, 2022, release 17. [Online]. Available: https://www.3gpp.org/ftp/Specs/archive/38_series/38.101-5
- [33] M. Asad Ullah, A. Heikkinen, M. Uitto, A. Anttonen, and K. Mikhaylov, "Impact of weather on satellite communication: Evaluating Starlink resilience," in 2025 IEEE 101st Vehicular Technology Conference (VTC2025-Spring), 2025, pp. 1–7.
- [34] International Telecommunication Union (ITU), "Recommendation ITU-R P.1410-6: Propagation data and prediction methods required for the design of terrestrial broadband radio access systems operating in a frequency range from 3 GHz to 60 GHz," ITU-R, Recommendation P.1410-6, Aug. 2023. [Online]. Available: https://www.itu.int/dms_pubrec/itu-r/rec/p/R-REC-P.1410-6-202308-I!!PDF-E.pdf
- [35] A. Al-Hourani, S. Kandeepan, and S. Lardner, "Optimal LAP altitude for maximum coverage," *IEEE Wireless Communications Letters*, vol. 3, no. 6, pp. 569–572, 2014.
- [36] H. Friis, "A note on a simple transmission formula," *Proceedings of the IRE*, vol. 34, no. 5, pp. 254–256, 1946.
- [37] 3rd Generation Partnership Project (3GPP), "NR; User Equipment (UE) conformance specification; Radio transmission and reception; Part 1: Range 1 standalone," 3GPP, Technical Specification (TS) 38.521-1, 2022, version 17.5.0, Release 17, ETSI TS 138 521-1 V17.5.0, under change control. [Online]. Available: <https://portal.3gpp.org/desktopmodules/Specifications/SpecificationDetails.aspx?specificationId=3381>
- [38] Federal Communications Commission (FCC), "Experimental License System Application (File No. 281537)," <https://apps.fcc.gov/els/GetAtt.html?id=281537&x=>, 2023, accessed: Feb. 2026.
- [39] SpaceX and T-Mobile, "Technical Narrative: Direct-to-Cellular Service," <https://cdn.arstechnica.net/wp-content/uploads/2023/05/SpaceX-T-Mobile-Technical-Narrative.pdf>, 2023, accessed: Feb. 2026.
- [40] 3rd Generation Partnership Project (3GPP), "Solutions for NR to Support Non-Terrestrial Networks (NTN)," 3GPP, Technical Report (TR) 38.821, 2020, release 16, under change control. [Online]. Available: <https://portal.3gpp.org/desktopmodules/Specifications/SpecificationDetails.aspx?specificationId=3525>